

Hybridization-Sensitive Fluorescent Probes for DNA and RNA by a Modular “Click” Approach

Julian Gebhard, Lara Hirsch, Christian Schwechheimer, and Hans-Achim Wagenknecht*



Cite This: *Bioconjugate Chem.* 2022, 33, 1634–1642



Read Online

ACCESS |



Metrics & More

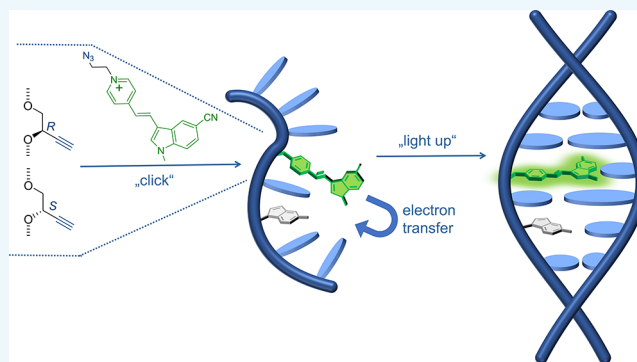


Article Recommendations



Supporting Information

ABSTRACT: Fluorescent DNA probes were prepared in a modular approach using the “click” post-synthetic modification strategy. The new glycol-based module and DNA building block place just two carbons between the phosphodiester bridges and anchor the dye by an additional alkyne group. This creates a stereocenter in the middle of this artificial nucleoside substitute. Both enantiomers and a variety of photostable cyanine–styryl dyes as well as thiazole orange derivatives were screened as “clicked” conjugates in different surrounding DNA sequences. The combination of the (*S*)-configured DNA anchor and the cyanylated cyanine–styryl dye shows the highest fluorescence light-up effect of 9.2 and a brightness of approximately $11,000 \text{ M}^{-1} \text{ cm}^{-1}$. This hybridization sensitivity and fluorescence readout were further



developed utilizing electron transfer and energy transfer processes. The combination of the hybridization-sensitive DNA building block with the nucleotide of 5-nitroindole as an electron acceptor and a quencher increases the light-up effect to 20 with the DNA target and to 15 with the RNA target. The fluorescence readout could significantly be enhanced to values between 50 and 360 by the use of energy transfer to a second DNA probe with commercially available dyes, like Cy3.5, Cy5, and Atto590, as energy acceptors at the 5'-end. The latter binary probes shift the fluorescent readout from the range of 500–550 nm to the range of 610–670 nm. The optical properties make these fluorescent DNA probes potentially useful for RNA imaging. Due to the strong light-up effect, they will not require washing procedures and will thus be suitable for live-cell imaging.

INTRODUCTION

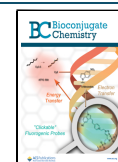
The complexity and diversity of biological RNA functions, not only for mRNA but also for any form of noncoding RNA, generates an increasing need for visualizing RNAs in living cells and organisms.^{1–4} One conventional methodology for measurement of expression levels of RNAs is quantitative real-time polymerase chain reaction (PCR), but this requires the lysis of the cells and tissues. More insights were gained by fluorescence in situ hybridization (FISH) with tagged probes.⁵ A slightly different but much more sensitive FISH method was developed later that allows to precisely image RNA transcripts by multiple (50–100) singly labeled, short oligonucleotide probes (20 nts) by single-molecule spectroscopy (e.g., smFISH) in fixed tissues.⁶ This method even allows the detection and quantification of RNAs at subcellular resolution in zebrafish embryos.^{7,8} Oligofluorophore labeling of the FISH probes reduces the total number needed for sensitive mRNA imaging.⁹ However, imaging of the short functional RNA pieces, including miRNAs, eRNAs, and other ncRNAs, in fixed or even in living cells still requires research on fluorogenic and hybridization-sensitive probes.¹⁰ Different concepts of fluorescent probes that give a light-up effect induced by hybridization to the target RNA include, for example, exciton-controlled hybridization-sensitive fluorescent oligonu-

cleotide (ECHO) probes,^{11,12} DNA/RNA “traffic lights”^{13,14} molecular beacons¹⁵ and forced intercalation thiazole orange (FIT) probes.^{16,17} These fluorescent oligonucleotide probes have one thing in common that they had to be prepared using individual DNA building blocks for each of the applied fluorophores. In principle, the copper(I)-catalyzed alkyne–azide cycloaddition (CuAAC) provides a much easier and more versatile synthetic access to fluorophore-modified oligonucleotides because any individual clickable DNA building block can be conjugated to different fluorophores. This allows the screening of a large number of potential fluorophores. This type of click chemistry has been established as a general synthetic tool for post-synthetic oligonucleotide modifications in vitro^{18,19} and recently applied for the preparation of super-sensitive multi-fluorophore FISH probes. However, those fluorescent probes were not hybridization

Received: May 26, 2022

Revised: July 11, 2022

Published: August 22, 2022



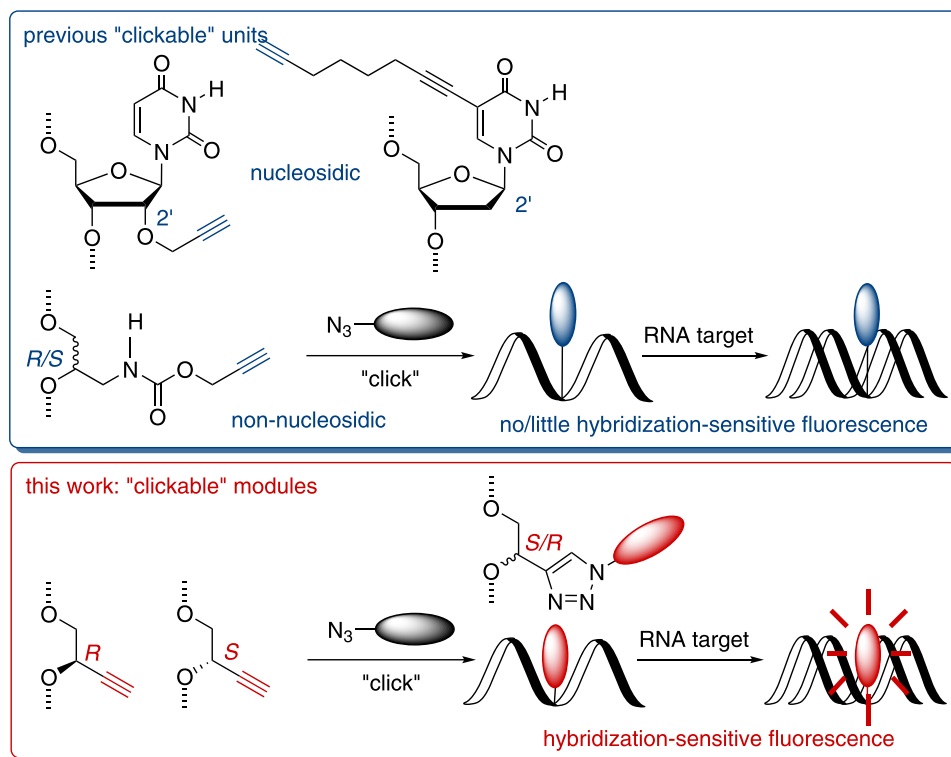


Figure 1. Change from nucleosidic to non-nucleosidic DNA building blocks with previous clickable ethynyl-modified modules and glycol-based module with clickable ethynyl group used in this work for hybridization-sensitive oligonucleotide probes.

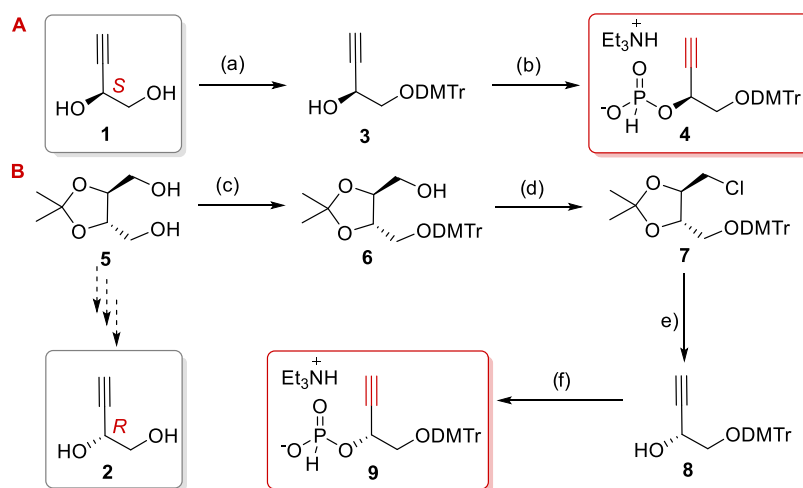


Figure 2. (A) (a) DMT-Cl, pyridine, r.t., overnight, 68%; (b) PCl_3 , *N*-methylmorpholine, 1,2,4-triazole, CH_2Cl_2 , 0 °C, 10 min, 69%. (B) (c) DMT-Cl, pyridine, r.t., overnight, 70%; (d) CCl_4 , PPh_3 , pyridine, 60 °C, 12 h, 77%; (e) LDA, tetrahydrofuran (THF), -78 to 0 °C, 3 h, 73%; and (f) PCl_3 , *N*-methylmorpholine, 1,2,4-triazole, CH_2Cl_2 , 0 °C, 10 min, 69%.

sensitive and require intensive washing steps for mRNA detection which limits their sensitivity and application to fixed cells. There are several promising approaches for RNA labeling in vitro and in cells based on click reactions.^{20,21} This includes the enzyme-directed incorporation of non-natural nucleotides, for instance, artificial nucleosides as “stealth” fluorescent labels,²² nucleosides with bio-orthogonally reacting groups for metabolic labeling,^{23–25} and chemo-enzymatic approaches for labeling RNAs for post-synthetic modifications.²⁶ Herein, we report new fluorescent oligonucleotide probes that are hybridization-sensitive and were prepared in a modular approach with a structurally simple building block using the

click post-synthetic modification strategy. The hybridization sensitivity and fluorescence readout with DNA and RNA were further developed utilizing electron transfer and energy transfer processes in combinations with second modifications.

RESULTS AND DISCUSSION

General Concept. Thiazol orange and several dyes of the cyanine–styryl type typically show enhanced fluorescence intensity by interaction with or intercalating into DNA.²⁷ Furthermore, the cyanine–styryl dyes are highly photostable and show a large Stokes shift.^{28,29} Both have significant advantages for fluorescence imaging of mRNA in cells or

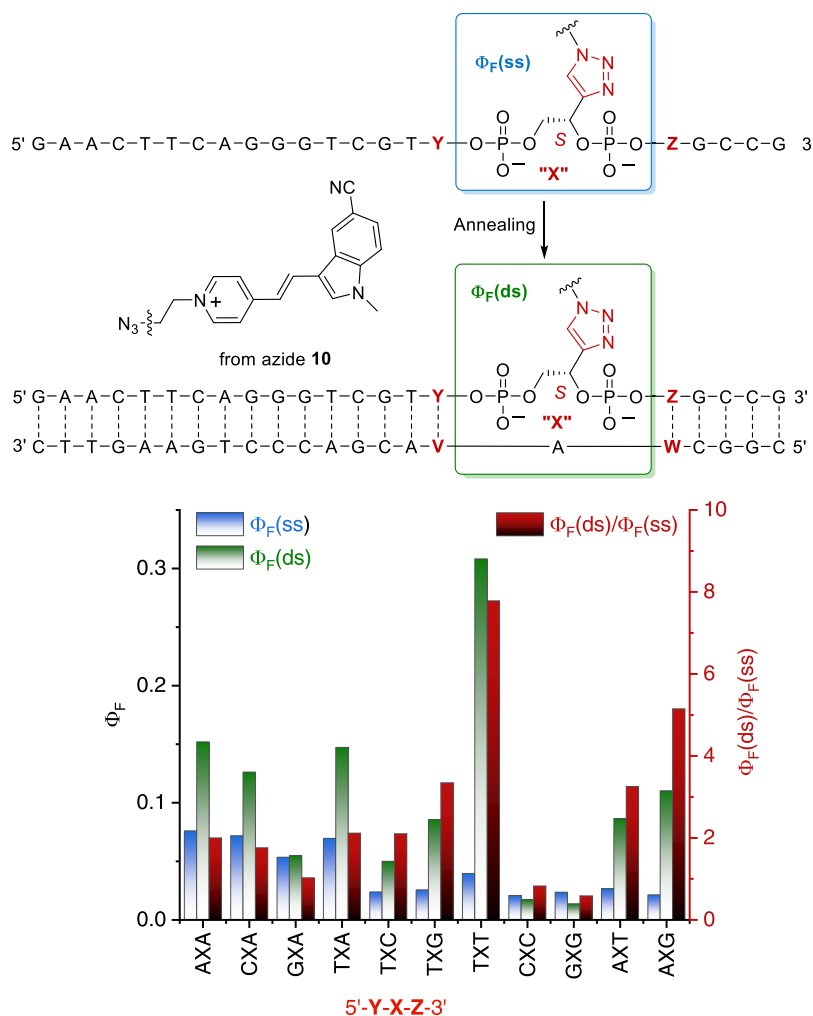


Figure 3. Left: Sequences of the DNA probes modified with the label X by “clicking” linker 1 to dye azide 10 in the variable region 5′-Y-X-Z-3′ and sequences of the complementary DNA (V and W are the canonical “counterbases” to Y and Z). Right: Fluorescence quantum yields $\Phi_F(ss)$ of the DNA single strands, fluorescence quantum yields $\Phi_F(ds)$ of the double-stranded DNA, and the ratios $\Phi_F(ds)/\Phi_F(ss)$ to quantify the light-up effect. 2.5 μ M DNA probe, 2.5 μ M DNA target, 10 mM NaPi buffer, 250 mM NaCl, pH 7, 20 °C, λ_{exc} = 450 nm.

tissues. Therefore, we decided to use these types of dyes to evaluate the hybridization sensitivity of our synthetic oligonucleotide probes. To gain hybridization sensitivity we assume that the dye has to be “clicked” close to the phosphodiester backbone via a short linker locating the dye in the proximity or even inside the DNA base stack.³⁰ The known clickable nucleosides with propargyl groups in the 2′ or 3′ positions do not follow this principle (Figure 1). In former work, we already showed that 2′-deoxyribofuranoside can be replaced by a clickable acyclic linker³¹ using both enantiomers.³² Glycol is the smallest possible connection between the phosphodiester bridges as evidenced by the glycol nucleic acids (GNAs).³³ To place the dyes into the DNA base stack, we designed the clickable components 1 with the (S)-configuration and 2 with the (R)-configuration at the central carbon atom. We investigated both enantiomers for the aimed hybridization sensitivity in different sequence contexts.

Synthesis of the Clickable DNA Building Blocks 4 and 9. The clickable DNA modules 1 and 2 differ only by their configurations at the branching carbon center (Figure 2). All our attempts failed to synthesize DNA with phosphoramidites of 1 or 2 as building blocks for automated solid-phase synthesis. We suppose that the nonbonding electron pair of the

P(III) in phosphoramidite reacts with the triple bond and prohibits its use in conventional oligonucleotide synthesis.^{34,35} Therefore, we synthesized both clickable units, with (S)- and (R)-configurations, as H-phosphonates 4 and 9 for automated DNA synthesis. The syntheses could partially be based on literature procedures and were therefore straightforward. For linker 1 with the (S)-configuration,^{36,37} the synthesis is completely according to the known literature procedure and we followed those procedures.^{38–40} Linker 1 was subsequently protected at the primary hydroxy function with the DMT group in 68% yield using the standard procedure. Finally, 3 was converted to H-phosphonate 4 in 69% yield. For linker 2 with the (R)-configuration,⁴¹ the known literature procedure^{37,42,43} was altered using DMT as the protecting group instead of Bn. Accordingly, the isopropylidene-protected starting compound 5 was protected by the DMT group at one of its primary hydroxy functions. The other hydroxy function remains unprotected in 6 and was converted into chloride 7. Double elimination of 7 gave the DMT-protected linker 8 in 73% yield, which was finally converted into the H-phosphonate 9 as a DNA building block.

The fluorescent oligonucleotide probes were prepared using automated DNA chemistry. The H-phosphonate chemistry⁴⁴

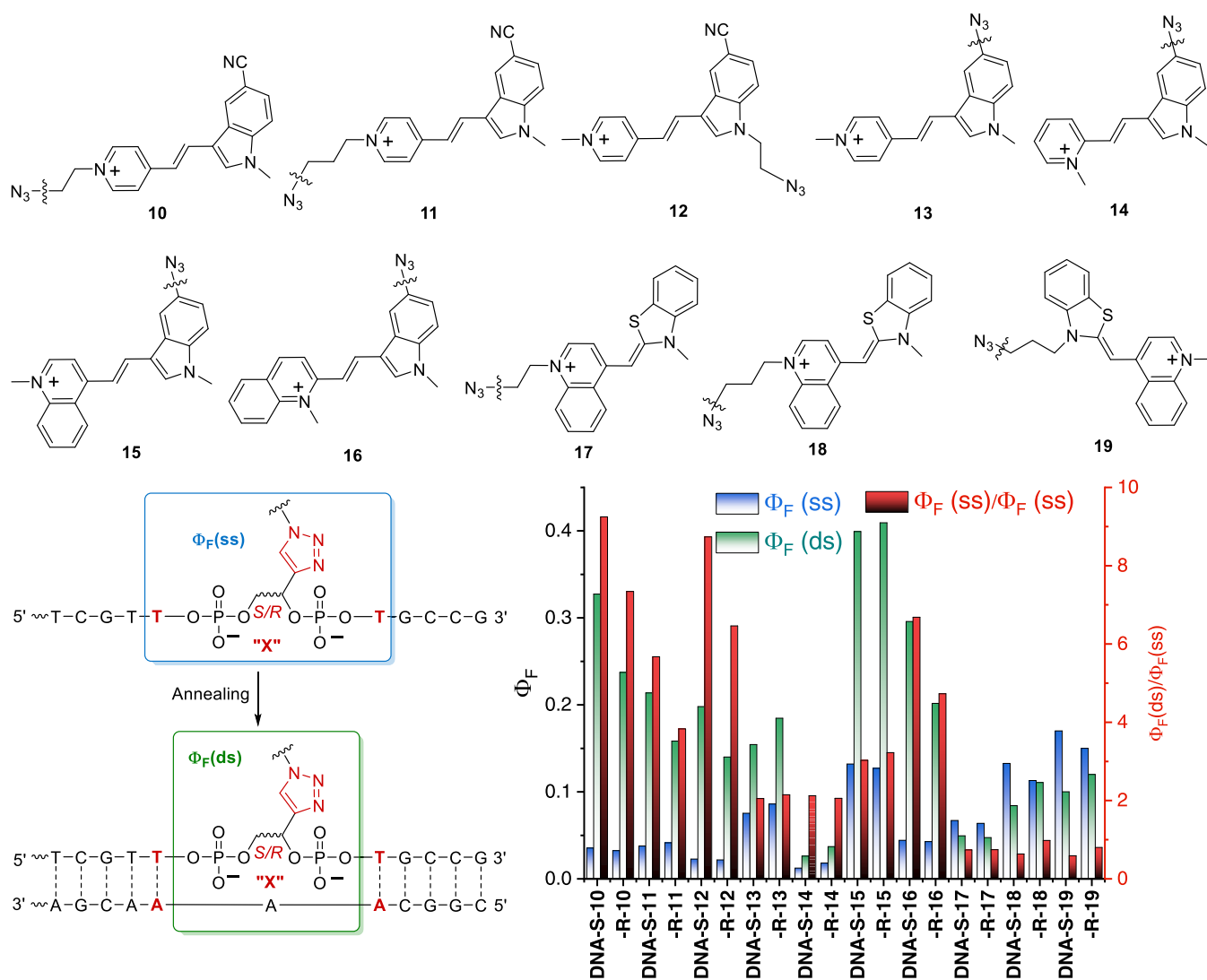


Figure 4. Left panel: Dye azides **10**–**19** used to modify the DNA probes DNA-S-**10**–DNA-R-**19** with X in the optimized region 5′-T-X-T-3′ and annealing with complementary DNA. Right panel: Fluorescence quantum yields $\Phi_F(ss)$ of the DNA single strands, fluorescence quantum yields $\Phi_F(ds)$ of the double-stranded DNA, and the ratios $\Phi_F(ds)/\Phi_F(ss)$ to quantify the light-up effect; 2.5 μ M DNA probe, 2.5 μ M DNA target, 10 mM NaPi buffer, 250 mM NaCl, pH 7, 20 °C, for λ_{exc} refer to λ_{max} in Table 1.

was solely applied for the coupling of the DNA building blocks **4** and **9** in combination with phosphoramidite chemistry for coupling of the conventional monomers A, C, G, and T, similar to the known literature procedures.⁴⁵ After deprotection and cleavage from the solid support, the synthesized oligonucleotides were separated from the reaction mixtures by DMT-affinity columns. The fluorescent dyes provide an azide functionality that reacts specifically with the alkyne-modified oligonucleotides in a CuAAC (click chemistry). After post-synthetic labeling according to our published click procedure,⁴⁶ the oligonucleotides were treated with ethylenediaminetetraacetic acid (EDTA) to remove copper salt impurities, purified by semi-preparative reversed-phase high-performance liquid chromatography (RP-HPLC), identified by matrix-assisted laser desorption/ionization-time of flight (MALDI-TOF) mass spectrometry, and quantified by UV/Vis absorption at 260 nm (see the Supporting Information).

Optimization of the Fluorescence Readout for Hybridization. The DNA base pairs adjacent to the fluorescent probe typically influence the spectroscopic properties of the dye.^{24,47,48} For this reason, the first experiments

aimed to evaluate the sequence dependence of the fluorescent readout and identify the optimal sequence environment(s) representatively for the combination of the linker **1** with the (S)-configuration and the dye from azide **10** in the center of short DNA pieces (abbreviated with “X” in Figure 3). This dye is a blue-green-emitting analogue of our recently developed clickable dyes with very high photostability.^{49,50} The other parts of the sequence of the oligonucleotide probes were chosen randomly. The “counterbase” to the modification site was A in this set of experiments. The different sequence variations both at the 3′- and the 5′-side of the fluorophore modification were compared to the fluorescence quantum yield of the single strand $\Phi_F(ss)$ vs the fluorescence quantum yield of the double-stranded hybrid $\Phi_F(ds)$ after annealing at high temperature (90 °C). The light-up effect was quantified by the ratio $\Phi_F(ds)/\Phi_F(ss)$ (Figure 3). The highest light-up of 9.3 was achieved for the sequence 5′-T-X-T-3′, followed by 7.8 for 5′-A-X-G-3′ and 3.4 for 5′-T-X-G-3′ and 5′-A-X-T-3′. All other combinations gave light-up values below 3.

We screened a set of pyridinium and quinolinium styryl-indole dyes **10**–**16** based on our recently developed clickable

Table 1. Spectroscopic Data of Fluorescent Probes DNA-S-10–DNA-R-19

DNA	T_m (°C)	λ_{\max} (nm)	$\epsilon_{\max}^{\text{ds}}$ (ds) ($10^3 \text{ M}^{-1} \text{ cm}^{-1}$)	λ_{em} (ss) (nm)	Φ_F (ss)	Φ_F (ds)	$\Phi_F(\text{ds})/\Phi_F(\text{ss})$	$B = \epsilon_{\max}^{\text{ds}} \Phi_F(\text{ds})$ ($10^3 \text{ M}^{-1} \text{ cm}^{-1}$)	Stokes shift (cm^{-1})
DNA-S-10	72	450	34	520	0.04	0.33	9.2	11	2990
DNA-R-10	72	450	35	520	0.03	0.24	7.3	8.3	2990
DNA-S-11	72	450	26	520	0.04	0.21	5.7	5.6	2990
DNA-R-11	71	450	20	520	0.04	0.16	3.8	3.2	2990
DNA-S-12	73	420	20	500	0.02	0.20	8.7	3.9	3810
DNA-R-12	73	420	20	500	0.02	0.14	6.5	2.8	3810
DNA-S-13	74	440	24	520	0.08	0.15	2.0	3.6	3500
DNA-R-13	73	440	23	520	0.09	0.18	2.1	4.2	3500
DNA-S-14	73	420	16	500	0.01	0.03	2.1	0.4	3810
DNA-R-14	73	420	16	500	0.02	0.04	2.1	0.6	3810
DNA-S-15	75	500	28	580	0.13	0.40	3.0	11	2760
DNA-R-15	74	500	28	580	0.13	0.41	3.2	11	2760
DNA-S-16	75	480	32	550	0.04	0.30	6.7	9.3	2650
DNA-R-16	74	480	32	550	0.04	0.20	4.7	6.4	2650
DNA-S-17	72	485	86	530	0.07	0.05	0.7	4.2	1750
DNA-R-17	72	485	86	530	0.06	0.05	0.7	4.0	1750
DNA-S-18	73	485	88	530	0.13	0.08	0.6	7.4	1750
DNA-R-18	74	485	96	530	0.11	0.11	1.0	11	1750
DNA-S-19	72	485	80	530	0.17	0.10	0.6	8.0	1750
DNA-R-19	71	485	86	530	0.15	0.12	0.7	9.9	1750

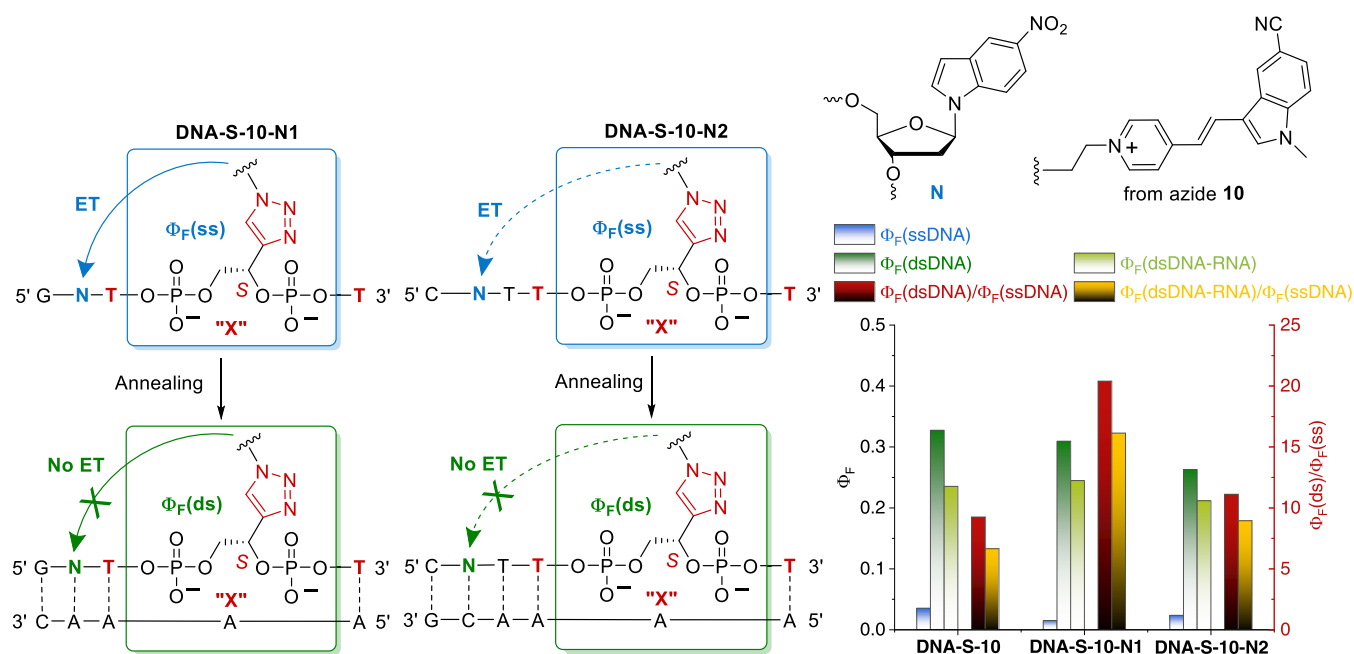


Figure 5. Left panel: DETEQ concept applied for DNA-S-10-N1 and DNA-S-10-N2. The electron transfer (ET) between X and N quenches the fluorescence of the single strands but not of the double strands upon annealing. Right panel: Fluorescence quantum yields $\Phi_F(\text{ss})$ of the DNA single strands, fluorescence quantum yields $\Phi_F(\text{ds})$ of the double-stranded DNA and DNA–RNA hybrids, and the ratios $\Phi_F(\text{ds})/\Phi_F(\text{ss})$ to quantify the light-up effect; 2.5 μM DNA probe, 2.5 μM DNA or RNA target, 10 mM NaP_i buffer, 250 mM NaCl, pH 7, 20 °C, $\lambda_{\text{exc}} = 450 \text{ nm}$.

dyes with very high photostability,^{49,50} in addition to thiazole orange derivatives 17–19. The dyes were synthesized based on literature procedures,^{51–54} and the synthesis details are described in the [Supporting Information](#). All dyes were clicked to the (S)-configured module 1 and the (R)-configured module 2, both as nucleotide-analogue components X in oligonucleotides with the optimized sequence 5'-T-X-T-3' at the modification site. We used A again as the counterbase to the modification site since this showed a light-up effect for both the (S)- and the (R)-configured linker. We measured again the fluorescence quantum yield of the single strand

$\Phi_F(\text{ss})$ vs the fluorescence quantum yield of the double-stranded DNA $\Phi_F(\text{ds})$ after annealing at high temperature, and the light-up effect was again quantified by the ratio $\Phi_F(\text{ds})/\Phi_F(\text{ss})$ (Figure 4). Furthermore, the optical data are listed in Table 1 including the brightness B. At first glance, the configuration of the linker at modification site X does not significantly alter the optical properties. However, a more careful examination of the optical properties reveals, that the (S)-configured anchor yields a slightly higher light-up effect. For instance, for the dye from azide 10, the ratio $\Phi_F(\text{ds})/\Phi_F(\text{ss})$ is 9.2 for DNA-S-10 in comparison to 7.3 for DNA-R-

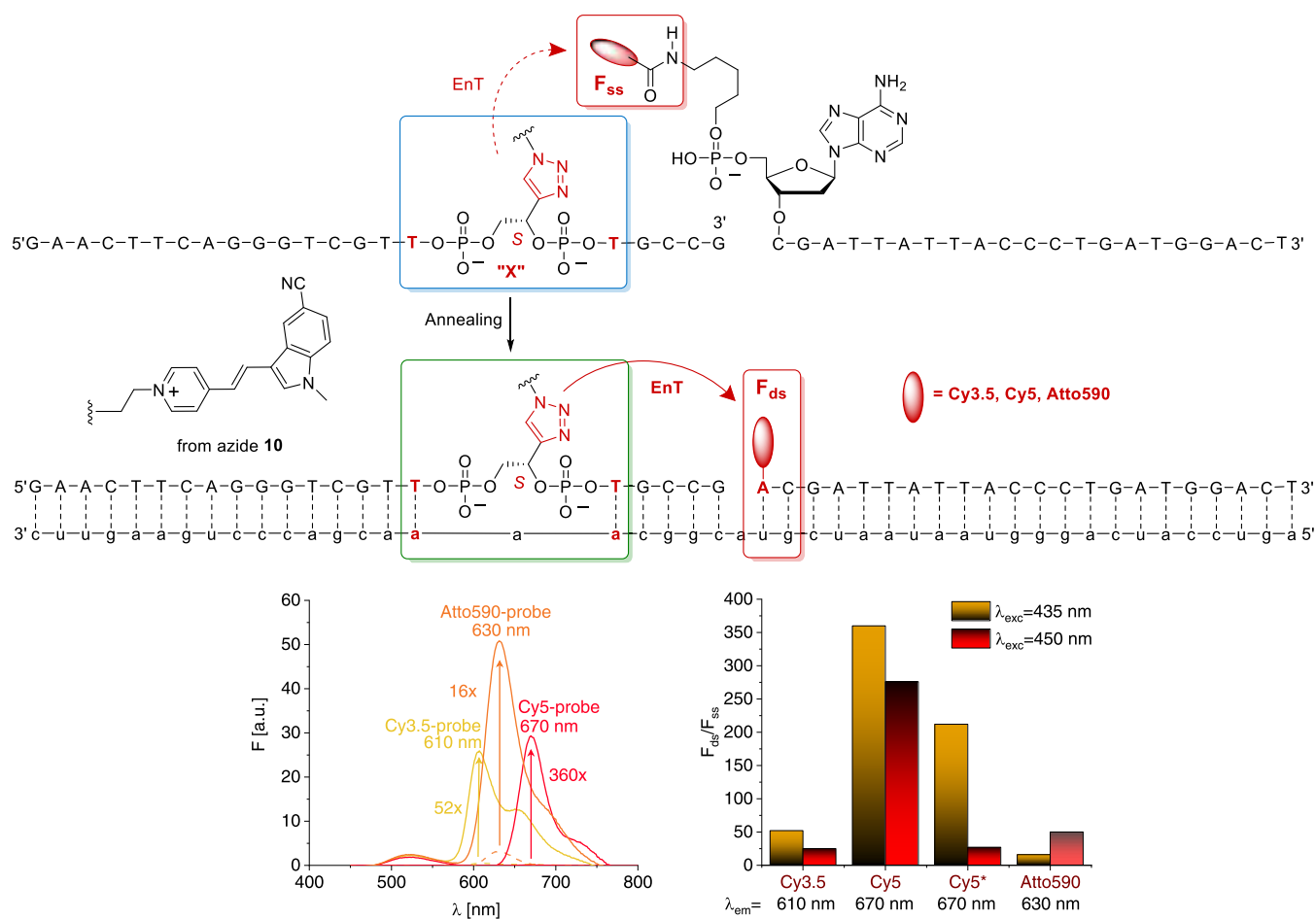


Figure 6. Combination of the hybridization-sensitive probe DNA-S-10 with energy transfer (EnT). The second probe is modified with Cy3.5, Cy5, and Atto590 as energy acceptors at the 5' end (illustrated in red). Bottom left panel: Fluorescence intensity changes detected with the different binary probes; $\lambda_{\text{exc}} = 435$ nm. Bottom right panel: Fluorescence intensity ratios between unbound DNA probes F_{ss} and target RNA-bound probes F_{ds} ; 2.5 μM DNA probe, 2.5 μM RNA target, 10 mM NaPi buffer, 250 mM NaCl, pH 7, 20 $^{\circ}\text{C}$, $\lambda_{\text{exc}} = 435/450$ nm. *The DNA-S-15 probe was used (instead of DNA-S-10) and excited at a wavelength of 450 nm or 500 nm.

10. This difference could be rationalized by the right-handed helicity of the DNA double helix. This is supported by the fact that the configuration-dependent difference in the quantum yield is observed only for double-stranded DNA probes, not for single-stranded probes. The dye from azide 11 shows a smaller light-up effect (5.7 for DNA-S-11 and 3.8 for DNA-R-11), which was expected since the elongated spacer with three CH_2 units between the dye and the oligonucleotide anchor moves the dye further away from the core DNA base stack and thus allows more conformational flexibility. If the dye was anchored by the nitrogen of the indole moiety (DNA-S-12 and DNA-R-12), the light-up effect was only slightly diminished (8.7 for DNA-S-11 and 6.5 for DNA-R-11) in comparison to DNA-R-10 and DNA-S-10, but the brightness B was significantly lower. In the dye azides 13–16, the alkyl spacer was completely omitted, and the azide was directly attached to the chromophore at the indole moiety, thereby replacing the cyano group. These dyes differ in the pyridinium and quinolinium parts, respectively. In this set of DNA probes, only DNA-S-16 and DNA-R-16 showed a significant light-up effect of 6.7 and 4.7, respectively, if at all. Since thiazole orange was a very often used dye in hybridization-sensitive DNA probes,^{24,47,48,55,56} we also tested three thiazole orange-derived dye azides, 17–19, bearing spacers of two different lengths. Unexpectedly, those three dyes did not show any light-up

effect when attached to DNA probes, which we cannot explain based on their structures. Furthermore, the Stokes shift for these DNA probes is only 10 nm, which is not meaningful for fluorescence RNA imaging purposes. The melting temperatures of all duplexes DNA-S-10 to DNA-R-19 lie in the narrow range between 71 and 75 $^{\circ}\text{C}$, and do not correlate with the observed light-up effect. This indicates that the light-up effect is not the simple result of stacking inside the DNA/RNA duplex, but results from a complex mixture of different effects, including stacking and photophysical interactions. In summary, the combination of the (*S*)-configured anchor and the dye from azide 10 in DNA-S-10 shows the highest light-up effect of nearly one order of magnitude and a suitable brightness of more than 11,000 $\text{M}^{-1} \text{cm}^{-1}$; we used that for further improvement of the fluorescence properties.

Combination with the DETEQ Concept Using 5-Nitroindole as a Fluorescence Quencher. In our earlier work, we established the “DETEQ” concept (“detection by electron transfer-controlled emission quenching”) for fluorescent DNA probes, which uses the defined quenching of fluorescence by electron transfer processes.⁵⁷ As one example of this concept we showed that 5-nitroindole quenches the fluorescence of dyes in DNA single strands, but not in DNA double strands if the 5-nitroindole moiety is placed near the fluorescent DNA modification.⁵⁸ We combined this quenching

concept with the hybridization-sensitive probe **DNA-S-10** that was the result of sequence optimization in the previous part (Figure 5). The 2'-deoxynucleoside of nitroindole (**N**) is commercially available as phosphoramidite and is considered as a universal base analogue since there is no significant base-pairing selectivity with one of the canonical DNA bases A, C, G, or T.⁵⁹ We placed the 5-nitroindole nucleotide at two different distances at the 5' site of the dye labeling site **X**, with one (**N1**) and two (**N2**) intervening T–A pairs. As expected, the light-up effect of the fluorescence from the single-stranded to the double-stranded DNA was enhanced. This was the result of a significant lowering of the fluorescence quantum yield of the single strand. These stands are in agreement with our proposed mechanism according to our DETEQ concept. Accordingly, the electron transfer in the single strand occurs between the dye and the 5-nitroindole as a quencher over a short distance by the flexible folding. After annealing to the double strand, the electron transfer is inhibited by the increased distance. The comparison of the fluorescence properties of the DNA double strands shows this characteristic behavior. The light-up effect on the fluorescence by hybridization is 9 without the nitroindole for **DNA-S-10**. With a distance of only one intervening base pair between **X** and **N** in **DNA-S-10-N1**, the fluorescence light-up effect increases to 20, whereas **DNA-S-10-N2** with two intervening base pairs between **X** and **N** shows a lower light-up effect of 11. For the later mRNA imaging application, we also checked the hybridization properties of these DNA probes with RNA. In the DNA–RNA hybrids, the light-up effect is increased from 7 (with **DNA-S-10**) over 9 (with **DNA-S-10-N2**) to 16 with **DNA-S-10-N2**. Here again, just one intervening base pair places **X** and **N** in the right position for optimal hybridization sensitivity of the fluorescence readout. The latter value is clearly in a range that will be suitable for fluorescent mRNA imaging in cell biology.

Combination in Binary Probes Using Energy Transfer.

Binary oligonucleotide probes with two different fluorescent labels have the general advantage that a fluorescence readout is obtained only if both probes bind to the RNA target and thereby come into proximity of 10 nm or closer to each other, which is in the range of typical Förster radii of dye combinations.⁶⁰ The energy transfer quenches the donor emission of the first probe upon its excitation and generates a wavelength-shifted fluorescence of the acceptor emission of the second probe. This concept was applied for mRNA imaging in single living cells.⁶¹ The use of a nonradiative⁶² or “dark”⁶³ intermolecular resonance energy transfer increases the fluorescence readout since spectral overlaps between the donor and acceptor emission typically generate poor signal-to-noise ratios. It looked therefore reasonable to combine our hybridization-sensitive probes in a binary probe concept together with a variety of fluorescent dyes as potential energy acceptors. In the single-stranded probe **DNA-S-10** nonradiative decay pathways dominate and there is only a low fluorescence intensity detectable. As a result of hybridization to the DNA or RNA target, these nonradiative pathways are suppressed and fluorescence is turned on by 1 magnitude of order, as described above. The suppression of nonradiative decay pathways should also pave the way for energy transfer if the donor emission overlaps with the absorbance of an acceptor dye in the second probe (Figure 6).

The change in the fluorescence intensity was measured using excitation at 435 nm, which is the characteristic wavelength for

the dye from azide **10** as an energy donor in these binary probes. The fluorescence readout was measured at the typical ranges of the acceptor dyes (with a fluorescence maximum of 610 nm for Cy3.5, 670 nm for Cy5, and 630 nm for Atto590). All three dyes have a very low extinction at 435 nm; nevertheless, there is a very small amount of background fluorescence F_{ss} detectable by direct excitation of these dyes. More importantly, the fluorescence F_{ds} is significantly intensified by the presence of complementary RNA and the probe **DNA-S10** in the ternary complex. The fluorescence intensity increases by a factor F_{ds}/F_{ss} of 52 (for the DNA probe with Cy3.5; $\lambda_{exc} = 435$ nm), 360 (for Cy5; $\lambda_{exc} = 435$ nm), and 50 (for Atto590; $\lambda_{exc} = 450$ nm). If the dye from azide **15** was used in **DNA-S-15** together with a Cy5-binary probe, the fluorescence intensity increases by a factor F_{ds}/F_{ss} of 212 (excitation at 450 nm). These contrast ratios for the acceptor emission are significantly larger than the contrast ratio achieved for the donor emission with **DNA-S-10** alone (9–10). This makes it clear that the fluorescence readout is significantly enhanced by the use of binary probes. The fluorescence contrast ratios are at least comparable or even better than reported values for similar DNA probes in the literature, like the FIT^{64,65} or DRET probes.⁶³

CONCLUSIONS

Fluorescent oligonucleotide probes were prepared by a modular approach using the click post-synthetic modification strategy. The new glycol-based DNA building block is probably the smallest possible clickable unit and nucleotide replacement, with just two carbons between the phosphodiester bridges and an additional alkyne group. Both enantiomers of this DNA building block and a variety of photostable cyanine–styryl dyes, as well as thiazole orange derivatives were screened in different sequential contexts. The combination of the (*S*)-configured DNA anchor and the cyanine–styryl dye from azide **10** in **DNA-S-10** shows the highest fluorescence light-up effect of nearly one order of magnitude and a suitable brightness of more than $11,000 \text{ M}^{-1} \text{ cm}^{-1}$. This hybridization sensitivity and fluorescence readout were further developed utilizing electron transfer and energy transfer processes. The combination with the nucleotide of 5-nitroindole as an electron acceptor and a quencher in a distance with one intervening base pair increases the light-up effect to 20 with the DNA target and 16 with the RNA target. The fluorescence light-up effect as the readout could be significantly enhanced by the use of a second DNA probe with commercially available dyes, like Cy3.5, Cy5, and Atto590, at the 5'-end. Using this binary probe concept, fluorescence contrast ratios in the range between 50 and 360 were obtained. The latter values were obtained with a red-shifted fluorescence readout from the range of 500–550 nm to the range of 610–670 nm. Taken together, these new fluorescent DNA probes have a significant potential for RNA imaging in live cells which do not require washing procedures. Additionally, they have the advantage that they can be synthesized in a modular approach using click chemistry, which makes the exchange of dyes to adjust the fluorescent readout for a given biological imaging problem easy.

EXPERIMENTAL PROCEDURES

All experimental details are described in the [Supporting Information](#).

■ ASSOCIATED CONTENT

SI Supporting Information

The Supporting Information is available free of charge at <https://pubs.acs.org/doi/10.1021/acs.bioconjchem.2c00241>.

Synthesis and characterization of the linker compounds, dyes, and modified oligonucleotides, including images of $^1\text{H}/^{13}\text{C}$ NMR and MS of synthesized compounds, and HPLC analytical traces and MS of modified oligonucleotides (PDF)

■ AUTHOR INFORMATION

Corresponding Author

Hans-Achim Wagenknecht – Karlsruhe Institute of Technology (KIT), Institute of Organic Chemistry, 7631 Karlsruhe, Germany; orcid.org/0000-0003-4849-2887; Email: Wagenknecht@kit.edu

Authors

Julian Gebhard – Karlsruhe Institute of Technology (KIT), Institute of Organic Chemistry, 7631 Karlsruhe, Germany

Lara Hirsch – Karlsruhe Institute of Technology (KIT), Institute of Organic Chemistry, 7631 Karlsruhe, Germany

Christian Schwechheimer – Karlsruhe Institute of Technology (KIT), Institute of Organic Chemistry, 7631 Karlsruhe, Germany

Complete contact information is available at: <https://pubs.acs.org/10.1021/acs.bioconjchem.2c00241>

Notes

The authors declare no competing financial interest.

■ ACKNOWLEDGMENTS

Financial support from the Deutsche Forschungsgemeinschaft (DFG, grant Wa 1386/17-2 and Graduiertenkolleg GRK 2039/2) and KIT is gratefully acknowledged.

■ REFERENCES

- (1) Rau, K.; Rentmeister, A. Making the Message Clear: Concepts for mRNA Imaging. *ACS Cent. Sci.* **2017**, *3*, 701–707.
- (2) Xia, Y.; Zhang, R.; Wang, Z.; Tian, J.; Chen, X. Recent advantages in high-performance fluorescent and bioluminescent RNA imaging probes. *Chem. Soc. Rev.* **2017**, *46*, 2824–2843.
- (3) Armitage, B. B. A. Imaging of RNA in live cells. *Curr. Opin. Chem. Biol.* **2011**, *15*, 806–812.
- (4) Ray, S.; Widom, J. R.; Walter, N. G. Life under the Microscope: Single-Molecule Fluorescence Highlights the RNA World. *Chem. Rev.* **2018**, *118*, 4120–4155.
- (5) Levisky, J. M.; Singer, R. H. Fluorescence in situ hybridization: past, present and future. *J. Cell. Sci.* **2003**, *116*, 2833–2838.
- (6) Raj, A.; Bogaard, P.; Rifkin, S. A.; Oudenaarden, A.; Tyagi, S. Imaging individual mRNA molecules using multiple singly labeled probes. *Nat. Methods* **2008**, *5*, 877–879.
- (7) Oka, Y.; Sato, T. N. Whole-mount single molecule FISH method for zebrafish embryo. *Sci. Rep.* **2015**, *5*, No. 8571.
- (8) Stapel, L. C.; Lombardot, B.; Broaddus, C.; Kainmueller, D.; Jug, F.; Myers, E. W.; Vastenhouw, N. L. Automated detection and quantification of single RNAs at cellular resolution in zebrafish embryos. *Development* **2015**, *143*, 540–546.
- (9) Raddaoui, N.; Croce, S.; Geiger, F.; Borodavka, A.; Möckel, L.; Stazzoni, S.; Viverge, B.; Bräuchle, C.; Frischmuth, T.; Engelke, H.; Carell, T. Supersensitive Multifluorophore RNA-FISH for Early Virus Detection and Flow-FISH by Using Click Chemistry. *ChemBioChem* **2020**, *21*, 2214–2218.
- (10) Hövelmann, F.; Seitz, O. DNA Stains as Surrogate Nucleobases in Fluorogenic Hybridization Probes. *Acc. Chem. Res.* **2016**, *49*, 714–723.
- (11) Guo, L.; Okamoto, A. Fluorescence-switching RNA for detection of bacterial ribosomes. *Chem. Commun.* **2017**, *53*, 9406–9409.
- (12) Okamoto, A. ECHO probes: a concept of fluorescence control for practical nucleic acid sensing. *Chem. Soc. Rev.* **2011**, *40*, 5815–5828.
- (13) Holzhauser, C.; Wagenknecht, H.-A. “DNA Traffic Lights”: Concept of Wavelength-Shifting DNA Probes and Application in an Aptasensor. *ChemBioChem* **2012**, *13*, 1136–1138.
- (14) Holzhauser, C.; Liebl, R.; Goepferich, A.; Wagenknecht, H.-A.; Breunig, M. RNA “Traffic Lights”: An Analytical Tool to Monitor siRNA Integrity. *ACS Chem. Biol.* **2013**, *8*, 890–894.
- (15) Tyagi, S.; Kramer, F. R. Molecular Beacons: Probes that Fluoresce upon Hybridization. *Nat. Biotechnol.* **1996**, *14*, 303–308.
- (16) Knoll, A.; Kankowski, S.; Schöllkopf, S.; Meier, J. C.; Seitz, O. Chemo-biological mRNA imaging with single nucleotide specificity. *Chem. Commun.* **2019**, *55*, 14817–14820.
- (17) Hövelmann, F.; Bethge, L.; Seitz, O. Single Labeled DNA FIT Probes for Avoiding False-Positive Signaling in the Detection of DNA/RNA in qPCR or Cell Media. *ChemBioChem* **2012**, *13*, 2072–2081.
- (18) Gramlich, P. M. E.; Wirges, C. T.; Manetto, A.; Carell, T. Postsynthetic DNA Modification through the Copper-Catalyzed Azide–Alkyne Cycloaddition Reaction. *Angew. Chem., Int. Ed.* **2008**, *47*, 8350–8358.
- (19) Fantoni, N. Z.; El-Sagheer, A. H.; Brown, T. A Hitchhiker’s Guide to Click-Chemistry with Nucleic Acids. *Chem. Rev.* **2021**, *121*, 7122–7154.
- (20) Schulz, D.; Rentmeister, A. Current Approaches for RNA Labeling in Vitro and in Cells Based on Click Reactions. *ChemBioChem* **2014**, *15*, 2342–2347.
- (21) Mannack, L. V. J. C.; Eising, S.; Rentmeister, A. Current techniques for visualizing RNA in cells. *Fluorescence* **2016**, *5*, 775.
- (22) Baladi, T.; Nilsson, J. R.; Gallud, A.; Celauro, E.; Gasse, C.; Levi-Acobas, F.; Sarac, I.; Hollenstein, M.; Dahlén, A.; Esbjörner, E. K.; Wilhelmsson, L. M. *J. Am. Chem. Soc.* **2021**, *143*, 5413–5424.
- (23) Ganz, D.; Harijan, D.; Wagenknecht, H.-A. *RSC Chem. Biol.* **2020**, *1*, 86–97.
- (24) Loehr, M. O.; Luedtke, N. W. A Kinetic and Fluorogenic Enhancement Strategy for Labeling of Nucleic Acids. *Angew. Chem., Int. Ed.* **2022**, *61*, No. e202112931.
- (25) Kubota, M.; Nainar, S.; Parker, S. M.; England, W.; Furche, F.; Spitale, R. C. Expanding the Scope of RNA Metabolic Labeling with Vinyl Nucleosides and Inverse Electron-Demand Diels-Alder Chemistry. *ACS Chem. Biol.* **2019**, *14*, 1698–1707.
- (26) Bollu, A.; Peters, A.; Rentmeister, A. Chemo-Enzymatic Modifications of the 5’-Cap to Study mRNAs. *Acc. Chem. Res.* **2022**, *55*, 1249–1261.
- (27) Sundström, V.; Gillbro, T. Viscosity dependent radiationless relaxation rate of cyanine dyes. A picosecond laser spectroscopy study. *Chem. Phys.* **1981**, *61*, 257–269.
- (28) Bohländer, P. R.; Wagenknecht, H.-A. Synthesis of a Photostable Energy-Transfer Pair for “DNA Traffic Lights”. *Eur. J. Org. Chem.* **2014**, *2014*, 7547–7551.
- (29) Bohländer, P. R.; Wagenknecht, H.-A. Synthesis and evaluation of cyanine–styryl dyes with enhanced photostability for fluorescent DNA staining. *Org. Biomol. Chem.* **2013**, *11*, 7458–7462.
- (30) Hövelmann, F.; Gaspar, I.; Chamiolo, J.; Kasper, M.; Steffen, J.; Ephrussi, A.; Seitz, O. LNA-enhanced DNA FIT-probes for multicolour RNA imaging. *Chem. Sci.* **2016**, *7*, 128–135.
- (31) Berndt, S.; Herzig, N.; Kele, P.; Lachmann, D.; Li, X.; Wolfbeis, O. S.; Wagenknecht, H.-A. Comparison of a nucleosidic vs. a non-nucleosidic postsynthetic “Click” modification of DNA with base-labile fluorescent probes. *Bioconjugate Chem.* **2009**, *20*, 558–564.
- (32) Lachmann, D.; Berndt, S.; Wolfbeis, O. S.; Wagenknecht, H.-A. Synthetic incorporation of Nile Blue into DNA using 2-deoxyribose

- substitutes: Representative comparison of (R)- and (S)-amino-propanediol as an acyclic linker. *Beilstein J. Org. Chem.* **2010**, *6*, 13.
- (33) Meggers, E.; Zhang, L. Synthesis and Properties of the Simplified Nucleic Acid Glycol Nucleic Acid. *Acc. Chem. Res.* **2010**, *43*, 1092–1102.
- (34) Collet, H.; Calas, P.; Commeyras, A. Influence of a perfluorobutyl substituent on the rearrangement of prop-2-ynyl diethylphosphites to allenic phosphonates. *J. Chem. Soc., Chem. Commun.* **1984**, 1152–1153.
- (35) Christov, V. C.; Ivanova, J. G. Bifunctionalized Allenes, VII: Two Methods for One-Pot Synthesis of Sulfonyl-Functionalized Allenecarboxylates and Phosphorylated Allenes. *Synth. Commun.* **2006**, *36*, 2231–2244.
- (36) Ralston, K. J.; Ramstadius, H. C.; Brewster, R. C.; Niblock, H. S.; Hulme, A. N. Self-Assembly of Disorazole C1 through a One-Pot Alkyne Metathesis Homodimerization Strategy. *Angew. Chem.* **2015**, *127*, 7192–7196.
- (37) Raji Reddy, C.; Rao, N. N.; Sujitha, P.; Kumar, C. G. Total Synthesis of (+)-Aspicilin by an Alkyne-Based Approach and Its Biological Evaluation. *Eur. J. Org. Chem.* **2012**, *2012*, 1819–1824.
- (38) Gooding, O. W.; Beard, C. C.; Jackson, D. Y.; Wren, D. L.; Cooper, G. F. Enantioselective formation of functionalized 1,3-disubstituted allenenes: synthesis of alpha-allenic omega-carbomethoxy alcohols of high optical purity. *J. Org. Chem.* **1991**, *56*, 1083–1088.
- (39) Kojima, N.; Maezaki, N.; Tominaga, H.; Asai, M.; Yanai, M.; Tanaka, T. Systematic construction of a monotetrahydrofuran library in annonaceous acetogenins by asymmetric alkynylation and stereodivergent tetrahydrofuran-ring formation. *Chem. - Eur. J.* **2003**, *9*, 4980–4990.
- (40) Patalag, L. J.; Jones, P. G.; Werz, D. B. BOIMPYs: Rapid Access to a Family of Red-Emissive Fluorophores and NIR Dyes. *Angew. Chem., Int. Ed.* **2016**, *55*, 13340–13344.
- (41) S Yadav, J.; Chander, M. C.; Joshi, B. V. An expeditious approach for the synthesis of optically active acetylenic alcohols. *Tetrahedron Lett.* **1988**, *29*, 2737–2740.
- (42) Lopp, M.; Kanger, T.; Miiraus, A.; Pehka, T.; Lille, Ü. Synthesis of a novel four-carbon chiron - (R)-1-t-butyltrimethylsilyl-3, 4-epoxy-but-1-yne. *Tetrahedron: Asymmetry* **1991**, *2*, 943–944.
- (43) Barbazanges, M.; Meyer, C.; Cossy, J.; Turner, P. Synthesis of 1,2-Amino Alcohols by Sigmatropic Rearrangements of 3-(N-Tosylamino)allylic Alcohol Derivatives. *Chem. - Eur. J.* **2011**, *17*, 4480–4495.
- (44) Froehler, B. C.; Ng, P. G.; Matteucci, M. D. Synthesis of DNA via deoxynucleoside H-phosphonate Intermediates. *Nucleic Acids Res.* **1986**, *14*, 5399–5407.
- (45) Schwöglar, A.; Carell, T. Toward Catalytically Active Oligonucleotides: Synthesis of a Flavin Nucleotide and Its Incorporation into DNA. *Org. Lett.* **2000**, *2*, 1415–1418.
- (46) Schwechheimer, C.; Doll, L.; Wagenknecht, H.-A. Synthesis of Dye-Modified Oligonucleotides via Copper(I)-Catalyzed Alkyne Azide Cycloaddition Using On- and Off-Bead Approaches. *Curr. Protoc. Nucleic Acid Chem.* **2018**, *72*, 4.80.1–4.80.13.
- (47) Klimkowski, P.; De Ornellas, S.; Singleton, D.; El-Sagheer, A. H.; Brown, T. Design of thiazole orange oligonucleotide probes for detection of DNA and RNA by fluorescence and duplex melting. *Org. Biomol. Chem.* **2019**, *17*, 5943–5950.
- (48) Ikeda, S.; Kubota, T.; Kino, K.; Okamoto, A. Sequence Dependence of Fluorescence Emission and Quenching of Doubly Thiazole Orange Labeled DNA: Effective Design of a Hybridization-Sensitive Probe. *Bioconjugate Chem.* **2008**, *19*, 1719–1725.
- (49) Schwechheimer, C.; Röncke, F.; Schepers, U.; Wagenknecht, H.-A. A new structure-activity relationship for cyanine dyes to improve photostability and fluorescence properties for live cell imaging. *Chem. Sci.* **2018**, *9*, 6557–6563.
- (50) Bohländer, P. R.; Wagenknecht, H.-A. Bright and photostable cyanine-styryl chromophores with green and red fluorescence color for DNA staining. *Methods Appl. Fluoresc.* **2015**, *3*, No. 044003.
- (51) Brown, A. S.; Bernal, L.-M.; Micotto, T. L.; Smith, E. L.; Wilson, J. N. Fluorescent neuroactive probes based on stilbazolium dyes. *Org. Biomol. Chem.* **2011**, *9*, 2142–2148.
- (52) Deligeorgiev, T. G.; Gadjev, N. I.; Drexhage, K.-H.; Sabnis, R. W. Preparation of intercalating dye thiazole orange and derivatives. *Dyes Pigm.* **1995**, *29*, 315–322.
- (53) Wang, X.; Krull, U. J. Synthesis and fluorescence studies of thiazole orange tethered onto oligonucleotide: development of a self-contained DNA biosensor on a fiber optic surface. *Bioorg. Med. Chem. Lett.* **2005**, *15*, 1725–1729.
- (54) Qiu, J.; Wilson, A.; El-Sagheer, A. H.; Brown, T. Combination probes with intercalating anchors and proximal fluorophores for DNA and RNA detection. *Nucleic Acid Res.* **2016**, *44*, No. e138.
- (55) Hara, Y.; Fujii, T.; Kashida, H.; Sekiguchi, K.; Liang, X.; Niwa, K.; Takase, T.; Yoshida, Y.; Asanuma, H. Coherent Quenching of a Fluorophore for the Design of a Highly Sensitive In-Stem Molecular Beacon. *Angew. Chem., Int. Ed.* **2010**, *49*, 5502–5506.
- (56) Kovaliov, M.; Segal, M.; Kafri, P.; Yavin, E.; Shav-Tal, Y.; Fischer, B. Detection of cyclin D1 mRNA by hybridization sensitive NIC-oligonucleotide probe. *Biorg. Med. Chem.* **2014**, *22*, 2613–2621.
- (57) Wagenknecht, H.-A. Fluorescent DNA Base Modifications and Substitutes: Multiple Fluorophore Labeling and the DETEQ Concept. *Ann. N. Y. Acad. Sci.* **2008**, *1130*, 122–130.
- (58) Menacher, F.; Rubner, M.; Berndt, S.; Wagenknecht, H.-A. Thiazole Orange and Cy3: Improvement of Fluorescent DNA Probes with Use of Short Range Electron Transfer. *J. Org. Chem.* **2008**, *73*, 4263–4266.
- (59) Loakes, D.; Brown, D. M. 5-Nitroindole as an universal base analogue. *Nucleic Acid Res.* **1994**, *22*, 4039–4043.
- (60) Kolpashchikov, D. M. Binary Probes for Nucleic Acid Analysis. *Chem. Rev.* **2010**, *110*, 4709–4723.
- (61) Tsuji, A.; Koshimoto, H.; Sato, Y.; Hirano, M.; Sei-Iida, Y.; Kondo, S.; Ishibashi, K. Direct Observation of Specific Messenger RNA in a Single Living Cell under a Fluorescence Microscope. *Biophys. J.* **2000**, *78*, 3260–3274.
- (62) Cardullo, R. A.; Agrawal, S.; Flores, C.; Zamecnik, P. C.; Wolf, D. E. Detection of nucleic acid hybridization by nonradiative fluorescence resonance energy transfer. *Proc. Natl. Acad. Sci. U.S.A.* **1988**, *85*, 8790–8794.
- (63) Barnoin, G.; Shaya, J.; Richert, L.; Le, H.-N.; Vincent, S.; Guérineau, V.; Mély, Y.; Michel, B. Y.; Burger, A. Intermolecular dark resonance energy transfer (DRET): upgrading fluorogenic DNA sensing. *Nucleic Acid Res.* **2021**, *49*, No. e72.
- (64) Fang, G.-m.; Chamiolo, J.; Kankowski, S.; Hövelmann, F.; Friedrich, D.; Löwer, A.; Meier, J. C.; Seitz, O. A bright FIT-PNA hybridization probe for the hybridization state specific analysis of a C→U RNA edit via FRET in a binary system. *Chem. Sci.* **2018**, *9*, 4794–4800.
- (65) Hövelmann, F.; Gaspar, I.; Ephrussi, A.; Seitz, O. Brightness Enhanced DNA FIT-Probes for Wash-Free RNA Imaging in Tissue. *J. Am. Chem. Soc.* **2013**, *135*, 19025–19032.